

# Numerical Simulation of the Effect of the Array-hole Injection and Cavity Combustor on the Rotating Detonation Engine Performance

Xiaojian He\*, Xiangyang Liu, Jianping Wang

Center for Combustion and Propulsion, CAPT & SKLTCS, Department of Mechanics and Engineering Sciences, College of Engineering, Peking University

Beijing, China

## Abstract

The subject of this paper is to use the discrete fuel injection model to simulate the discontinuous distribution of reactants in rotating detonation engine experiments, and the cavity combustor is also utilized in simulation to get a deeper insight about the performance of the cavity RDE. Four kinds of injection patterns are employed with inlet-area ratio 44.5%, 49.8%, 54.7% and 100%, and four RDE models of different cavity depths are employed. In case\_C1h1 to case\_C1h4, we can draw the conclusion that the array-hole injection pattern is the dominant factor that leads to the multi-DWC modes, and when the array-hole count increases, the DWC is getting close to 1. As the inlet-area ratios  $\psi$  increases, the  $F_{sp}$  increase rate of model C4 is the highest initially, and later on it becomes the slowest, resulting in the lowest  $F_{sp}$  finally which is significantly less than that of cavity combustor, indicating the promising advantages of cavity RDE over traditional RDE in propulsive performance.

## 1 Introduction

In the numerical simulation of the rotating detonation engine (RDE), there are two different fuel-injection patterns, full-area injection and discrete injection. Full-area injection bringing continuous reactant into the combustor is extensively used in RDE numerical simulation for the sake of its simplicity, but it should be noted that the in actual RDE experiments the reactants are injected into the combustor through holes or slits, which means the reactant is distributed discontinuously. The discretely distributed fresh mixtures cannot continuously provide energy for detonation waves. Hence the detonation waves become weak and unstable. Compare these two simulation injection patterns with the case of the real experiments, the discrete injection is more close to reality. So these years the discrete injection patterns are paid more and more attention, and array-hole injection, one kind of the discrete injection patterns, is researched in this paper.

Besides, the structure of the combustor can bring huge effect to the detonation mode and flow-filed structure. Annular RDE combustor has been studied a lot and gained abundant amounts of knowledge about RDE combustion, and hollow RDE combustor has also been paid sufficient attention due to its benefit on stable detonation realization and simple structure. In addition, cavity combustor are widely utilized in scramjet to promote fuel mixing and stabilize flame. Inspired by the hollow chamber and the cavity in the scramjet, the annular cavity in CRD combustor has been proposed by Peng et al.[1] to improve detonation combustion organization and they did find some advantages in stable detonation realization by utilizing the cavity combustor RDE. And more attention should be paid on this newly proposed cavity RDE.

Thus, the subject of this paper is to use the discrete fuel injection model to simulate the discontinuous distribution of reactants in real rotating detonation engine experiments, and the cavity combustor is also utilized in simulation to get a deeper insight about the performance of the cavity RDE. Four kinds of injection patterns are employed with inlet-area ratio 44.5%, 49.8%, 54.7% and 100%, and four RDE models of different cavity depths are employed with depth 0.010 m, 0.0067 m, 0.0033 m and 0.

## 2 Computational Method

Detonation is a transient combustion phenomenon with multi-component chemical reactions. The unsteady and Favre-averaged compressible Navier–Stokes equations are solved by a set of conservative variables:

$$\frac{\partial \bar{\rho}}{\partial t} + \frac{\partial \bar{\rho} \tilde{u}_j}{\partial x_j} = 0 \quad (1)$$

$$\frac{\partial \bar{\rho} \tilde{u}_i}{\partial t} + \frac{\partial \bar{\rho} \tilde{u}_i \tilde{u}_j}{\partial x_j} = - \frac{\partial \bar{p}}{\partial x_i} + \frac{\partial}{\partial x_j} (\bar{\tau}_{ij} - \tau_{ij}^{sgs}) \quad (2)$$

$$\frac{\partial \bar{\rho} \tilde{E}}{\partial t} + \frac{\partial}{\partial x_j} [(\bar{\rho} \tilde{E} + \bar{p}) \tilde{u}_j] = \frac{\partial}{\partial x_j} \left[ \lambda \frac{\tilde{T}}{x_j} + \tilde{u}_i \bar{\tau}_{ij} - H_j^{sgs} + \sigma_j^{sgs} \right] + \bar{\omega}_T \quad (3)$$

$$\frac{\partial \bar{\rho} \tilde{Y}_k}{\partial t} + \frac{\partial \bar{\rho} \tilde{u}_j \tilde{Y}_k}{\partial x_j} = \frac{\partial}{\partial x_j} \left[ \bar{\rho} D \frac{\partial \tilde{Y}_k}{\partial x_j} - Y_{j,k}^{sgs} \right] + \bar{\omega}_k \quad (4)$$

In present study, the governing equations are solved with a OpenFOAM solver rhoHLLCFoam developed by our previous work [2]. The solver can well simulate discontinuities and cellular structure in detonation combustion. A two-step global chemical mechanism containing six species (KERO, O<sub>2</sub>, N<sub>2</sub>, CO, CO<sub>2</sub> and H<sub>2</sub>O) is used for KERO kinetics.

### 3 Physical Model

Four cavity RDE models of different cavity depths are employed with depth 0.010 m, 0.0067 m, 0.0033 m and 0, as listed in Fig.1, and we labeled them as C1, C2, C3 and C4. The combustor length for both cases is 4.0 cm, and the outer radius is 2.0cm. The inlet is on the left side, with several kinds of injection patterns, and the outlet is on the right side, with a full area exit.

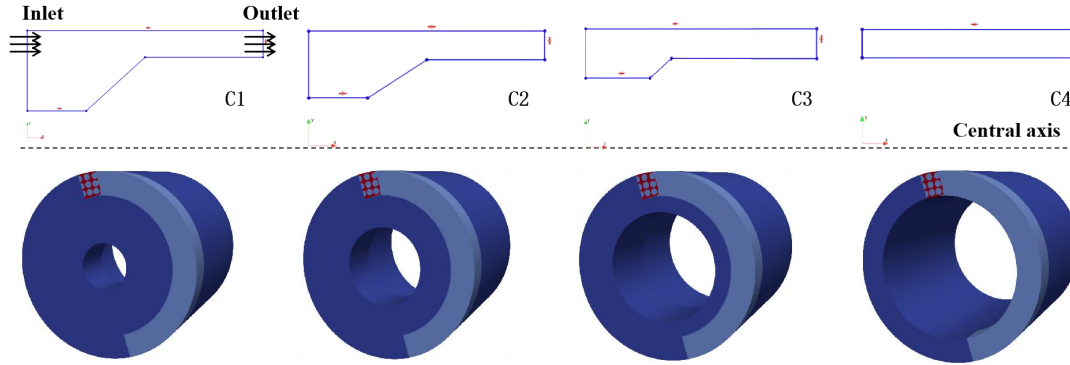


Fig.1 2D cross-section (upper) and 3D profile of cavity RDE models

In all four models, the outer region  $R > R_{inner}$ , as shown in Fig.2, on the injection surface is the fresh mixture intake area where the combustible premixed mixtures are fed into the chamber by three rows of array-holes or full-area. We define the inlet-area ratio  $\psi$  as  $A_{inlet}/(A_{inlet}+A_{wall})$ , with  $A_{inlet}$  the area of inlet surface and  $A_{wall}$  the area of rigid wall surface. So when the injection array-holes number is equal to 54, 60 and 66, the inlet-area ratios  $\psi$  is 44.5%, 49.8% and 54.7%, respectively, and we labeled them as h1, h2 and h3. And when the injection pattern is full-area injection, the inlet-area ratios  $\psi$  is 100%, labeled as h4. The smaller value of  $\psi$  leads to the bigger gap between reactant strips and more discrete distribution of reactants.

The inner region  $R < R_{inner}$  on the injection surface is solid wall. The radius of injector is 0.7 mm. To analyze the impact of array-hole injection model on detonation flow-field, we set several cases with full-area injection model for comparison as shown in Fig.2. The grid size 0.15 mm is enough to capture the wave structure in flow field. The total number of grid points is 210 million.

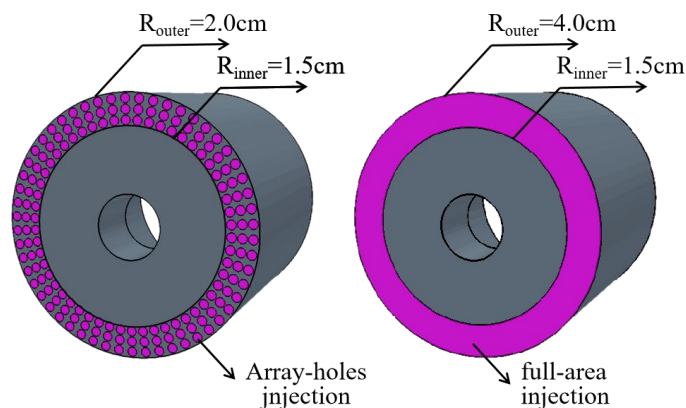


Fig.2 Schematic diagram of array-holes injection model (left) and full-area injection model (right)

Adiabatic, non-slip and non-catalytic boundary conditions are used on rigid wall surfaces. Premixed KERO/air mixtures are injected into the chamber through converging micro-nozzles at each grid point on inlet surface. The injection conditions ( $p$ ,  $T$ ,  $V$ ) are set assuming isentropic expansion through grid points into the combustion chamber. Based on the relation between micro-nozzle stagnation pressure

$p_0$  and the pressure on head-end wall  $p_w$ , the inlet situations can be divided into three cases: no injection, subsonic injection and sonic injection. The inlet stagnation pressure and temperature for all cases are 6 atm and 1300 K, respectively. To initialize the detonation flow-field, a hot-spot with pressure 50 atm and temperature 3500 K are set at bottom of combustion chamber at  $t = 0$  as shown in Fig. 1.

## 4 Result and discussion

### 4.1 The effects of array-holes injection

#### 4.1.1 Detonation waves count (DWC)

Fig. 3 shows the pressure gradient distribution in 2D computational domains within model C1 and C2 by extending a thin slice to a plane along azimuthal direction, with radius and height of the slice  $r = 1.85$  cm and  $h = 4.0$  cm, respectively. Azimuthal position is represented by  $r \cdot \theta$  along x-axis. Axial position is represented by  $h$  along y-axis. In case\_C1h1 to case\_C1h4, the detonation Waves count (DWC) is 4, 3, 3 and 1, respectively. To be specific, the detonation propagation mode is homo-rotating four waves, homo-rotating three waves, homo-rotating three waves (counter-clockwise), and one wave. It indicates that as the inlet-area ratios  $\psi$  increases, the DWC is decreasing. Compared array-hole injection with full-area injection, it seems that the array-hole injection causes multi-DWC modes (which means the DWC is more than 1). However, we also found that in these four cases the mass flowrates of cases with array-hole injection are lower than that of cases with full-area injection. According to our knowledge, the changes of injection patterns and the mass flowrates both can change the detonation mode, so we implemented case\_C1h5 to gain deeper insight into this ambiguous question. In case\_C1h5, the full-area injection pattern is employed and we reduced the initial pressure to decrease the reactant mass flowrate to match the levels of that in case\_C1h1 to case\_C1h3. The result shows that the detonation mode in case\_C1h5 is still one-wave mode, indicating the decrease of mass flowrate does not necessarily cause the presence of the multi-DWC modes. So in case\_C1h1 to case\_C1h4, we can reasonably draw the conclusion that the array-hole injection pattern is the dominant factor that leads to the multi-DWC modes, and when the array-hole count increases the discontinuity is reducing, and DWC is getting close to 1. Furthermore, it can be inferred that in real RDE experiments the discontinuous distribution of the reactant is one of the factors that result in multi-DWC modes.

Similarly, when it comes to the model C2, C3 and C4, array-hole injection brings multi-DWC modes and full-area injection brings one-wave mode. And the DWC decreases generally as the inlet-area ratios  $\psi$  increases from 44.5% to 100%, with a notable exception though: as the inlet-area ratios  $\psi$  increases from 44.5% to 54.7%, cases in model C2 exhibit the same homo-rotating 4 waves mode, which shows a promising subject that in some cavity combustors of special structures the mode changes little as reactant discontinuity changes. As we all know, reactant discontinuity change is very common in RDE and detracts the engine performance severely, so cavity combustors of low sensitivity to reactant discontinuity deserve further investigation and the detonation combustion is likely to be more stable in these kinds of combustors.

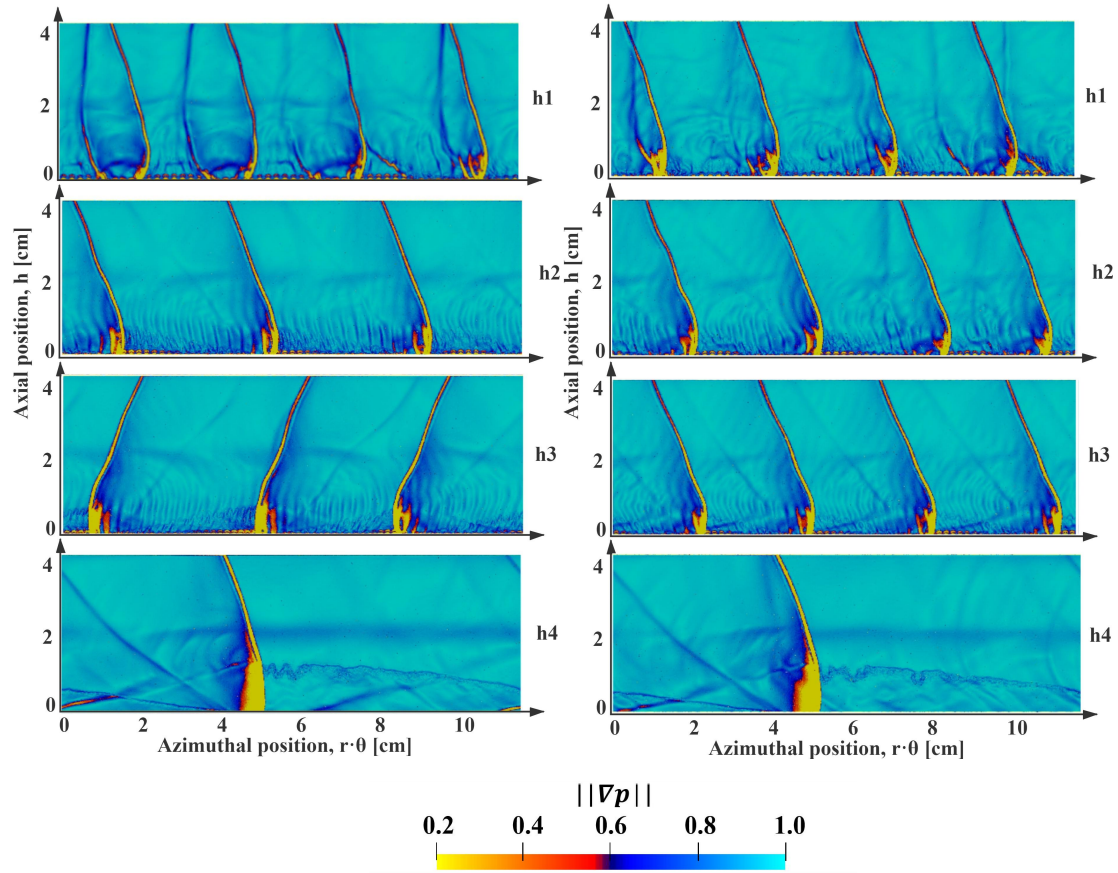


Fig.3 Pressure gradient distribution in slices at  $r = 1.85$  cm with  $\psi = 44.5\%$ ,  $49.8\%$ ,  $54.7\%$  and  $100\%$ . (Left) Model C1. (Right) Model C2. Logarithmic pressure gradient contour calculated as  $||\nabla p|| = \exp(-\frac{150 \cdot |\nabla p|}{p_{max}})$ .  $|\nabla p|$  is the pressure gradient.

#### 4.1.2 Propulsive Performance

The performance of engine in air-breathing configuration is described by the specific thrust in terms of oxidizer. Specific thrust gives a measure of oxidizer usage in the production of thrust. The detailed calculation formula can be found in our previous work [2].

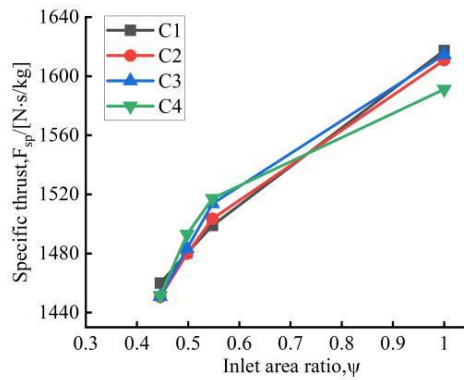


Fig.4 Specific thrust  $F_{sp}$  against inlet-area ratio  $\psi$

Fig.4 shows that as the inlet-area ratios  $\psi$  increases from 44.5% to 100%, the specific thrust ( $F_{sp}$ ) of all the four models C1 to C4 increases constantly from  $\sim 1460$  to  $\sim 1600$  N·s/kg. The  $F_{sp}$  increase rates of all the four models are fast at first and then become slow as  $\psi$  increases, similar phenomenon can be found in Liu et al.[3], though the detailed data are not close due to the different reaction equations and numerical methods utilized by this work and Liu et al.[3]. In addition, Fig.4 indicates that when inlet-area ratios  $\psi$  is low as 44.5%,  $F_{sp}$  of all the four models are close. The  $F_{sp}$  increase rate of model C4 is the highest initially, and later on it becomes the lowest, resulting in the lowest  $F_{sp}$  finally which is significantly less than that of cavity combustors, indicating the promising advantages of cavity RDE over traditional RDE in propulsive performance.

In addition, the effect of cavity combustor on the detonation mode, propulsive performance and flow-field were also studied in our work which are not exhibited in this extended abstract due to the limited length of the article.

## References

- [1] Peng H Y , Liu W D , Liu S J , et al. The effect of cavity on ethylene-air Continuous Rotating Detonation in the annular combustor[J]. International Journal of Hydrogen Energy, 2019, 44(26):14032-14043.
- [2] Liu X Y , Luan M Y , Chen Y L , et al. Propagation behavior of rotating detonation waves with premixed kerosene/air mixtures[J]. Fuel, 2021, 294(6):120253.
- [3] Liu X Y , Luan M Y , Chen Y L , et al. Flow-field analysis and pressure gain estimation of a rotating detonation engine with banded distribution of reactants[J]. International Journal of Hydrogen Energy, 2020.